RAPID COMMUNICATIONS

PHYSICAL REVIEW B VOLUME 38, NUMBER 4 1 AUGUST 1988

Observation of oxygen-vacancy-ordered domains in oxygen-deficient single-crystal $YBa_2Cu_3O_{6.7}$

C. H. Chen, D. J. Werder, L. F. Schneemeyer, P. K. Gallagher, and J. V. Waszczak
AT&T Bell Laboratories, Murray Hill, New Jersey 07974
(Received 31 May 1988)

Ordered domains due to oxygen vacancies in oxygen-deficient $YBa_2Cu_3O_{6.7}$ single crystals have been imaged by dark-field electron microscopy using the diffuse diffraction spots centered at $(\frac{1}{2},0,0)$. When projected along the c axis, the ordered domains have longitudinal and transverse dimensions of $\sim$200 and $\sim$20 Å, respectively. The longitudinal direction of the domains is parallel to the Cu-O chain direction (i.e., b axis). The vacancy-ordered domains are estimated to occupy $\lesssim$3% of the sample volume.

Recently it was shown how the oxygen stoichiometry affects the physical properties of the high-T_c superconductor $YBa_2Cu_3O_{7-x}$.[1] In that work ceramic samples in the range $0.3 \lesssim x \lesssim 0.4$ showed a sharp transition temperature at 60 K with a Meissner effect of $\sim$90%. A plateau in T_c and a minimum in room-temperature resistivity for the above range of x suggested the existence of oxygen-vacancy ordering. Well-defined superlatticelike diffuse diffraction peaks due to ordering have now been observed by electron[2-5] and, more recently, x-ray[6] diffraction studies. Depending on the details of the heat treatment process and the nominal oxygen stoichiometry in the oxygen-deficient material, various superlatticelike periodicities, such as $(\frac{1}{2},0,0)$, $(0,\frac{1}{2},0)$, $(\frac{1}{2},\frac{1}{2},0)$, $(\frac{2}{5},0,0)$, and $(\frac{1}{4},\frac{1}{4},0)$ have been observed. Real-space imaging of oxygen vacancies has so far been limited to high-resolution transmission electron microscopy.[7-10] It has been argued[10] that high-resolution lattice images are sensitive to the oxygen vacancies and the row containing the oxygen vacancies between Ba planes in the $YBa_2Cu_3O_7$ structure can be identified. However, the issue of the visibility of oxygen vacancies by high-resolution lattice images was brought under close scrutiny recently,[11,12] and it was concluded that fingerprinting the oxygen-vacancy ordering in high-resolution images would be extremely difficult and not very convincing.

In this Rapid Communication, we report real-space imaging of oxygen-vacancy-ordered domains (VOD) by dark-field transmission electron microscopy in the oxygen-deficient $YBa_2Cu_3O_{6.7}$ single crystals. The resolution of dark-field images is not nearly as good as high-resolution images, but their interpretation is simpler and more straightforward. We have observed, for the first time in $YBa_2Cu_3O_{7-x}$, the spatial fluctuation of vacancy ordering and decomposition. The VOD has longitudinal and transverse dimensions of $\sim$200 and $\sim$20 Å, respectively. The longitudinal direction of the VOD is found to be parallel to the b axis (i.e., the Cu-O chain direction). As a result of a decomposition reaction the VOD occupy only a fraction of the volume in the sample.

The preparation of oxygen-deficient $YBa_2Cu_3O_{6.7}$ single crystals has been described previously.[6] Briefly, the samples were made with nominal oxygen concentration of 6.7 by quenching from 667 °C in O_2. The single crystals with c axis normal to the surface have the form of a thin plate with $\sim$20–50 μm in thickness and 0.5–1 mm in cross section. These crystals showed[6] a superconducting transition temperature of 57 K and a dc flux exclusion of $\sim$25%. The samples for transmission electron microscopy were prepared by ion milling without a prior mechanical polishing step. A JEOL 2000 FX electron microscope operating at 200 kV was used for the present study.

In all the $YBa_2Cu_3O_{7-x}$ samples we have examined, including polycrystalline ceramics, single crystals, and epitaxial thin films, the size of twin domains were found to be more or less uniform in a particular sample. However, in the oxygen-deficient single crystals, there are areas in which very large twin domains ($\sim$1 μm) are separated by very small twins ($\sim$200 Å). The regular array of these alternating large and small twins is unusual and perhaps is due to a peculiar anisotropic local stress during the nucleation and growth process. Of course, there are areas where the twin boundaries are more equally spaced ($\lesssim$1000 Å). We did not, however, find any difference in these two types of areas as regards the oxygen-vacancy ordering.

In our previous study of oxygen-vacancy ordering in annealed ceramics of $YBa_2Cu_3O_{6.72}$, diffuse diffraction spots centered at $(\frac{1}{2},0,0)$ and $(\frac{2}{5},0,0)$ were observed.[3] In the present case, we have found only the $(\frac{1}{2},0,0)$ diffuse superlattice spots as shown in the electron diffraction pattern obtained from an area covering many twin domains (Fig. 1). However, the $(\frac{1}{2},0,0)$ diffuse superlattice peaks are more intense and less diffuse along the a axis than those observed in ceramic samples. Because of the small difference in lattice parameters of a and b, it is difficult, but not impossible, for electron diffraction to determine the direction of the ordering vector. Our measured ordering vector $(\frac{1}{2},0,0)$ is consistent with x-ray diffraction results[6] obtained from similar crystals grown in the same batch. The coherence length of the ordering along the a axis is estimated from the diffuse streaks to be $\sim$20 Å. The superlattice peaks have a narrow width along the b axis indicating a coherence length longer than 100 Å in this direction. Tilting the sample with respect to either the a or b axis, reveals that the diffuse superlattice spots have a rodlike shape running parallel to the c axis.

Fluctuations in vacancy ordering and variations in size (or shapes) of the VOD across a sample, which are unobservable in a diffraction pattern, can be obtained in real

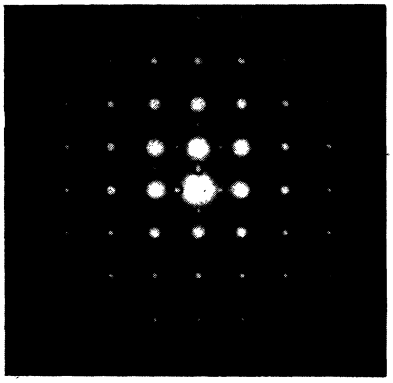

FIG. 1. Electron diffraction pattern obtained from an area covering many twin domains. The presence of $(\frac{1}{2},0,0)$ superlattice spots in both horizontal and vertical directions is due to twinning. The two circled $(\frac{1}{2},0,0)$ superlattice spots are those used to obtain dark-field images shown in Figs. 2(a) and 2(b).

space by dark-field imaging using the diffuse superlattice spots. The high intensity of the $(\frac{1}{2},0,0)$ superlattice peaks as shown in Fig. 1 makes dark-field imaging feasible. In Figs. 2(a) and 2(b), we show a pair of dark-field images obtained from the two diffuse streaks circled in Fig. 1. It is clear from Figs. 2(a) and 2(b) that every other twin domain is decorated with small domains of strong contrast which we identify as VOD. The complementary contrast between Figs. 2(a) and 2(b) is expected from the twinning relationship between two adjacent twin domains,

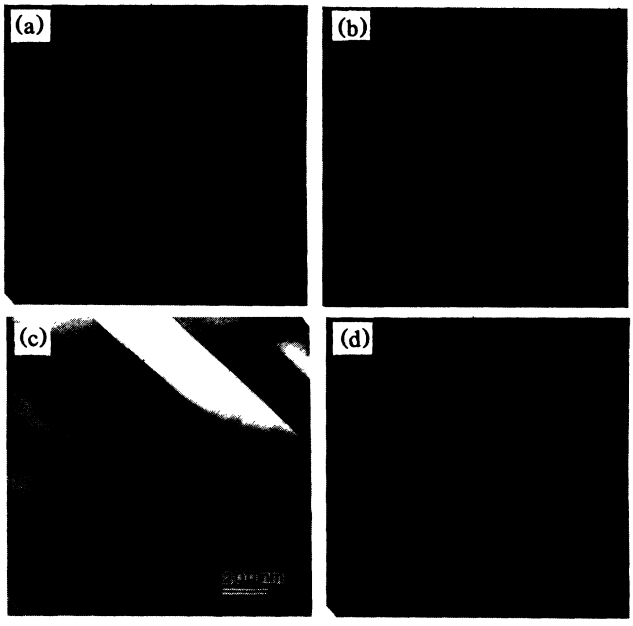

FIG. 2. (a) and (b) are dark-field images obtained from the two circled $(\frac{1}{2},0,0)$ superlattice spots shown in Fig. 1. Note that the longitudinal directions of the bright domains in (a) and (b) are perpendicular to each other. (c) is a dark-field image obtained from a main Bragg spot, and (d) is a magnified view of the boxed area shown in (a).

in that the *a* and *b* axes are rotated 90° across a twin boundary.[13] The longitudinal directions of the stringlike domains in Figs. 2(a) and 2(b), which coincide with the *b* axis (i.e., the Cu-O chain direction), are therefore perpendicular to each other. The VOD are visible in the dark-field images only when the $(\frac{1}{2},0,0)$ superlattice spots are used. Dark-field images obtained from the Bragg reflections of the parent lattice, as shown in Fig. 2(c), do not reveal this type of contrast. We, therefore, conclude that the small bright domains shown in Figs. 2(a) and 2(b) represent the shape of the VOD and indicate fluctuations of the vacancy ordering in the sample. We have also shown in Fig. 2(d) a magnified view of the VOD from the boxed area shown in Fig. 2(a). Because of the long exposure time required, the dark-field images shown in Fig. 1 were obtained with a moderate resolution. The resolution is determined mainly by the mechanical stability of the specimen holder during the exposure and is estimated to be $\lesssim 30$ Å. Of course, the resolution can be greatly improved by sacraficing the intensity. Close examination of the VOD shown in Fig. 2 reveals that the longitudinal dimensions of the VOD vary from ~ 100 to ~ 500 Å, with an average size of ~ 200 Å. This corresponds to the real-space coherence length of the vacancy ordering along the *b* axis. The transverse dimension of the VOD (i.e., along the *a* axis) is much smaller ranging from 15 to 50 Å, but nominally 20 Å as judged from dark-field images obtained with much shorter exposure time. The sizes and the orientation of the VOD would give rise to a diffuse diffraction peak which is broad along the *a* axis and narrow along the *b* axis, and this is exactly what is shown in Fig. 1. As we noted earlier, the superlattice peaks at $(\frac{1}{2},0,0)$ have a rodlike shape parallel to the *c* axis, suggesting the coherence length of the VOD along the *c* axis is on the order of the *c* axis lattice parameter (11.7 Å). Figures 2(a) and 2(b) were obtained with the *c* axis parallel to the electron beam since the intensity of the $(\frac{1}{2},0,0)$ superlattice peaks is at their maximum at this orientation. The VOD shown in Fig. 2, therefore, represent a superposition of all the VOD projected along the *c* axis through the whole thickness of the specimen and cannot reveal the dimension of VOD along the *c* axis. The contrast of the VOD will be greatly enhanced in the areas where VOD's overlap when projected along the *c* axis. Dark-field images of the same area obtained from various equivalent $(\frac{1}{2},0,0)$ superlattice spots show exactly the same arrangement of VOD indicating all the VOD are diffracting coherently and, that Figs. 2(a) and 2(b) actually exhibit *all* the VOD in that area. The dark regions between the VOD, therefore, represent areas where no oxygen-vacancy ordering has occurred. Nevertheless, it does not exclude the real possibility that oxygen vacancies still occur in the regions between VOD. If the periodicity of oxygen-vacancy ordering is determined by the oxygen stoichiometry, one would expect a vacancy ordering of $(\frac{1}{2},0,0)$ in $YBa_2Cu_3O_{7-x}$ for $x=0.5$ and $(\frac{1}{3},0,0)$ ordering for $x=0.33$. This would suggest that VOD have an oxygen stoichiometry of 6.5 which is different from the oxygen stoichiometry of 6.7 in the sample determined experimentally. Our observation, therefore, provides direct evidence for ordering and decomposition reactions in the off-stoichiometric YBa_2-

Cu_3O_{7-x}, which support the general idea of ordering and decomposition developed in a recent theoretical work by Khachaturyan and Morris.[14] In that theoretical treatment, ordering and decomposition reactions involving only $YBa_2Cu_3O_6$ and $YBa_2Cu_3O_7$ were considered. It would be of interest to extend that treatment to other ordering and decomposition reactions.

A rough estimate of the volume fraction of VOD can be obtained from Fig. 2(d). If we take the dimensions of a single VOD as $20\times200\times10$ Å, and the intensity of the VOD is proportional to the number of overlapping domains projected along the c axis through the whole thickness of the sample (~1000 Å), we find that the VOD occupy a volume fraction $\lesssim3\%$. The major uncertainties of this estimate come from the thickness of the sample and from the minimum detectable level of the VOD. We believe that the small volume fraction and the small sizes of the VOD observed in our experiment are indicative of a metastable, not a stable equilibrium phase of the $(\frac{1}{2},0,0)$ ordering. A recent theoretical phase diagram calculation,[15] however, has suggested that the $(\frac{1}{2},0,0)$ vacancy ordering is a stable equilibrium phase.

The relationship between VOD and superconducting properties is not totally clear at the present time. However, we note that the polycrystalline ceramics of $YBa_2Cu_3O_{6.72}$ exhibit a much stronger Meissner effect ($\sim90\%$) with a much weaker $(\frac{1}{2},0,0)$ diffuse peak.[3] In our single-crystalline sample, with a much stronger $(\frac{1}{2},0,0)$ diffuse peak, the Meissner effect is only $\sim20\%$. This seems to suggest that a large volume percentage of VOD are detrimental to the flux pinning in the superconductor.

Finally, we would like to present another interesting, but less commonly observed, finding which represents another ordering and decomposition reaction in the sample. In Fig. 3 we show a bright-field image of such an area which exhibits a modulated tweedlike structure with an average spacing of ~100 Å. No twinning structure can be found in this area as evidenced by the absence of splitting of diffraction spots due to twinning. A diffraction pattern obtained from a several-thousand-angstroms area is similar to that observed from a single twin domain in a typical $YBa_2Cu_3O_{7-x}$ sample. About each Bragg spot in the direction of the modulation is a diffuse intensity corresponding to a range of spacings. However, convergent beam electron diffraction with a fine probe reveals that the two orthorhombic axes a and b are not in the same direction as those in the crystal structure of $YBa_2Cu_3O_7$. The a and b axes, have in fact rotated 45° with respect to the well-known orthorhombic axes in $YBa_2Cu_3O_7$. The electron diffraction pattern can now be indexed by a new orthorhombic unit cell with dimensions $\sqrt{2}a_c\times\sqrt{2}a_c\times3a_c$

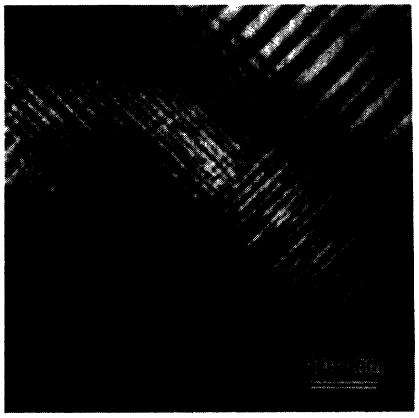

FIG. 3. A bright-field image showing a modulated tweedlike structure with a fine spacing ~100 Å.

where $a_c\simeq3.9$ Å is the lattice parameter of a cubic perovskite cell. The orientations of the modulated tweedlike structure shown in Fig. 3, however, are still parallel to the orientations of the twin boundaries observed in another area of the same sample. The modulated tweedlike structure, therefore, provides another way of minimizing the strain energy during the tetragonal-to-orthorhombic phase transition. Note that the modulation wave vectors are along the new a and b orthorhombic axes, unlike the twin boundaries which run parallel to the (110) direction in the $YBa_2Cu_3O_7$ structure. This type of contrast modulation resembles that observed in the spinodal decomposition of many metallic[16] or semiconducting[17] alloys. Modulation wave vectors in a spinodal system are expected to be parallel to the major symmetry directions which are elastically soft. The rarity with which this phase is observed indicates that it is a metastable phase and can be obtained by rapid quenching. This is the first time we have seen this modulated tweedlike structure in the high-T_c oxide superconductors. Experiments to understand the details of this modulated contrast are now underway.

In conclusion, we have observed an oxygen VOD in real space by dark-field imaging using the superlattice reflections due to vacancy ordering. The vacancy ordering is inhomogeneous spatially and should have a significant effect on the superconducting properties in the oxygen-deficient oxide superconductors. The microstructure resulting from the decomposition and vacancy ordering is very interesting by itself and may present another hurdle to the interpretation of many macroscopic physical measurement which assume spatial homogeneity.

We would like to thank B. Batlogg, R. M. Fleming, and J. Kwo for many useful discussions.

[1]R. J. Cava, B. Batlogg, C. H. Chen, E. A. Rietman, S. M. Zahurak, and D. J. Werder, Phys. Rev. B **36**, 5719 (1987).

[2]C. Chaillout, M. A. Alario-Franco, J. J. Capponi, J. Chenavas, J. L. Hodeau, and M. Marezio, Phys. Rev. B **36**, 7118 (1987).

[3]D. J. Werder, C. H. Chen, R. J. Cava, and B. Batlogg, Phys. Rev. B **37**, (1988).

[4]H. W. Zandbergen, G. Van Tendeloo, T. Okabe, and S. Amelinckx, Phys. Status Solidi (a) **103**, 45 (1987).

[5]M. Tanaka, M. Terauchi, K. Tsuda, and A. Ono, Jpn. J. Appl. Phys. (to be published).

[6]R. M. Fleming, L. F. Schneemeyer, P. K. Gallagher, B. Batlogg, L. W. Rupp, and J. V. Waszczak, Phys Rev. B **37**,

7920 (1988).
[7]Y. Syono, M. Kikuchi, K. Ohishi, K. Hiraga, H. Arai, Y. Matsui, N. Kobayashi, T. Sasoka, and Y. Muto, Jpn. J. Appl. Phys. **26**, L498 (1987).
[8]K. Hiraga, D. Shindo, M. Hirabayashi, M. Kikuchi, and Y. Syono, J. Electron Microsc. **36**, 261 (1987).
[9]R. Beyers, G. Lim, E. M. Engler, R. J. Savoy, T. M. Shaw, T. R. Dinger, W. J. Gallagher, and R. L. Sandstrom, Appl. Phys. Lett. **50**, 1918 (1987).
[10]A. Ourmazd, J. A. Rentschler, J. C. H. Spence, M. O'Keefe, R. J. Graham, D. W. Johnson, Jr., and W. W. Rhode, Nature **327**, 308 (1987).
[11]J. M. Gibson, Nature **329**, 763 (1987).
[12]N. P. Huxford, D. J. Eaglesham, and C. J. Humphreys, Nature **329**, 812 (1987).
[13]C. H. Chen, D. J. Werder, S. H. Liou, J. R. Kwo, and M. Hong, Phys. Rev. B **35**, 8767 (1987).
[14]A. G. Khachaturyan and J. W. Morris, Jr., Phys. Rev. Lett. **59**, 2776 (1987).
[15]L. T. Wille, A. Berera, and D. de Fontaine, Phys. Rev. Lett. **60**, 1965 (1988).
[16]J. W. Cahn, Trans. Metall. Soc. AIME **242**, 166 (1968).
[17]M. M. J. Treacy, J. M. Gibson, and A. Howie, Philos. Mag. A **51**, 389 (1985).

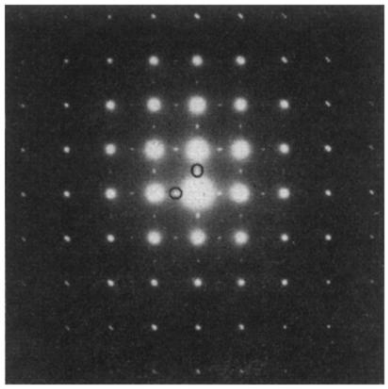

FIG. 1. Electron diffraction pattern obtained from an area covering many twin domains. The presence of $(\frac{1}{2},0,0)$ superlattice spots in both horizontal and vertical directions is due to twinning. The two circled $(\frac{1}{2},0,0)$ superlattice spots are those used to obtain dark-field images shown in Figs. 2(a) and 2(b).

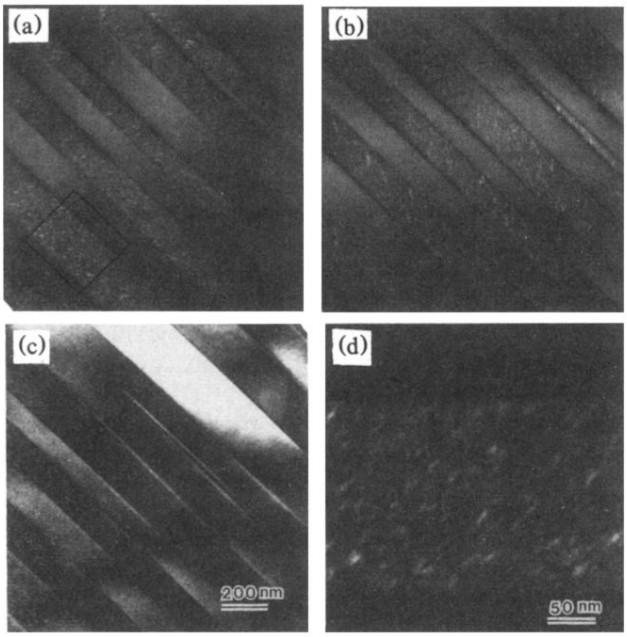

FIG. 2. (a) and (b) are dark-field images obtained from the two circled $(\frac{1}{2},0,0)$ superlattice spots shown in Fig. 1. Note that the longitudinal directions of the bright domains in (a) and (b) are perpendicular to each other. (c) is a dark-field image obtained from a main Bragg spot, and (d) is a magnified view of the boxed area shown in (a).

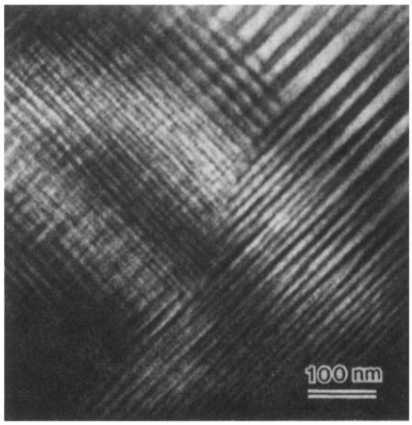

FIG. 3. A bright-field image showing a modulated tweedlike structure with a fine spacing $\sim$100 Å.